

Geometric resonance of bragg-reflected cyclotron orbits in unidirectional lateral superlattices: The role of harmonics of the potential modulation

Akira Endo*, Yasuhiro Iye

Institute for Solid State Physics, University of Tokyo, Kashiwa, Chiba 277-8581, Japan

Available online 17 April 2006

Abstract

A new class of small amplitude low-field magnetoresistance oscillation observed in a unidirectional lateral superlattice (ULSL) attributable to the geometric resonance of Bragg-reflected cyclotron orbits (open orbits) reveals the presence of higher harmonics in the potential modulation. By contrast, the commensurability oscillation (CO) exhibited by the same ULSL sample appears to be explicable by a formula taking only the fundamental component into consideration. The apparent inconsistency is ascribed to the difference in the sensitivity to the higher harmonics of the two types of magnetoresistance oscillations. The amplitude of the new oscillation is discussed in terms of the probability of the magnetic breakdown and the ratio of the distance traveled by the electrons during one period of the open orbit to the mean free path.

© 2006 Elsevier B.V. All rights reserved.

PACS: 73.23.–b; 73.23.Ad; 73.21.Cd

Keywords: Lateral superlattice; Bragg reflection; Magnetotransport; Magnetic breakdown

A unidirectional lateral superlattice (ULSL) represents a prototypical system of a two-dimensional electron gas (2DEG) with an artificially introduced modulation; there, the period and the amplitude of the introduced potential modulation give rise to intriguing phenomena through their interplay with the length and energy scales inherent in 2DEGs under a magnetic field. Well-known examples are the commensurability oscillation (CO) [1] and the positive magnetoresistance (PMR) [2]. Both CO and PMR can basically be understood in the framework of the semi-classical motion of the electrons under the modulated potential landscape. Although the study of superlattice was originally motivated by the possibility of designing man-made band structures (minibands and minigaps) having length and energy scales quite different from those of natural crystals [3], phenomena heralding the effect

resulting from minibands and minigaps was elusive in lateral superlattices until quite recently [4,5].

In a recent paper [6], the present authors reported a new class of small amplitude magnetoresistance oscillation superposed on PMR. The oscillation was ascribed to the geometric resonance between the period of the ULSL and the width of an open orbit resulting from the formation of the minigap. We observed the resonances of open orbits arising not only from the lowest-order Bragg reflection but also from the second- or third-order reflections. This implies, although not explicitly mentioned in Ref. [6], the presence of corresponding harmonics in the potential modulation. In the present paper, we discuss the sensitivity of the new oscillation to the higher harmonics in comparison with that of CO. We also discuss the intensity of the resonance in terms of the probability of magnetic breakdown and the scattering of electrons out of the open orbit.

ULSL samples for the present study are described in detail elsewhere [6]. Briefly, potential modulation was

*Corresponding author. Fax: +81 471 36 3301.

E-mail address: akrendo@issp.u-tokyo.ac.jp (A. Endo).

introduced by a grating of negative electron-beam resist placed on the surface via the strain-induced piezoelectric effect [7] to the 2DEG plane residing just below the AlGaAs/GaAs heterointerface at the depth $d = 90$ nm from the surface.

Fig. 1 illustrates a typical example of the new oscillation. The low-field magnetoresistance trace show PMR at $|B| < \sim 0.04$ T and CO outside the region. The upward slope of the PMR shows non-monotonic behavior barely discernible in the trace itself, but can be made evident either by subtracting slowly varying background or by taking the second derivative with respect to the magnetic field. We examined the positions of the minima in $(d^2/dB^2)(\Delta\rho_{xx}/\rho_0)$ for several ULSL samples with the period a ranging from 138 to 207 nm, and for the range of the electron density $n_e = 1.7\text{--}3.1 \times 10^{15} \text{ m}^{-2}$, and concluded that the oscillation results from the geometric resonance between a and the width of the open orbit [6,8].

Fig. 2 depicts the Fermi contour in the reciprocal space. The contour consists of multiple Fermi circles for free electrons each shifted by $2\pi n/a$ (n integer) in the k_x direction, with a gap opening up at the crossing of two circles, resulting in the open and closed orbits. The size of the gap between the n th nearest circles are determined by the n th harmonic content of the potential modulation V_n . (Strictly speaking, higher order terms of the fundamental component, V_1^n , can in principle also contribute to the n th gap for $n = 2, 3, \dots$ [9]. However, the effect is negligibly small for our small V_1). The modulation amplitudes are much smaller than the Fermi energy E_F , $\eta_n \equiv V_n/E_F \ll 1$, for all the ULSL samples for the present study. The size of the gap, Δk_n , in the k_y direction is given by, in the nearly free-electron approximation appropriate for small η_n (leaving out the effect of higher order terms mentioned

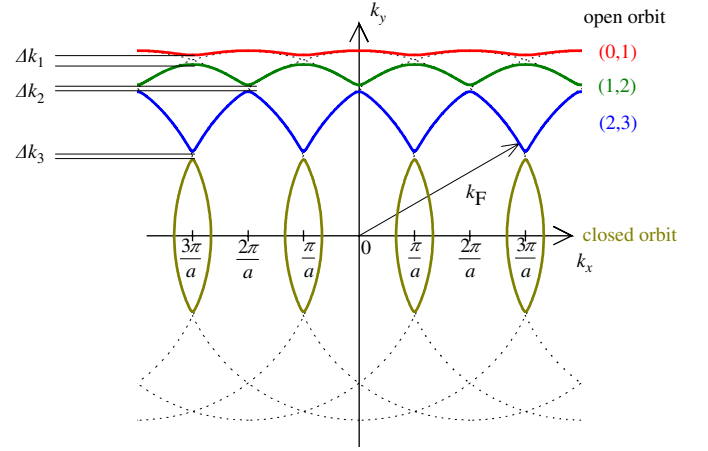


Fig. 2. Fermi contour showing open and closed orbits in the reciprocal space. The index (j, k) specifies an open orbit composed of the segments from the j th and k th nearest Fermi circles for the free electrons.

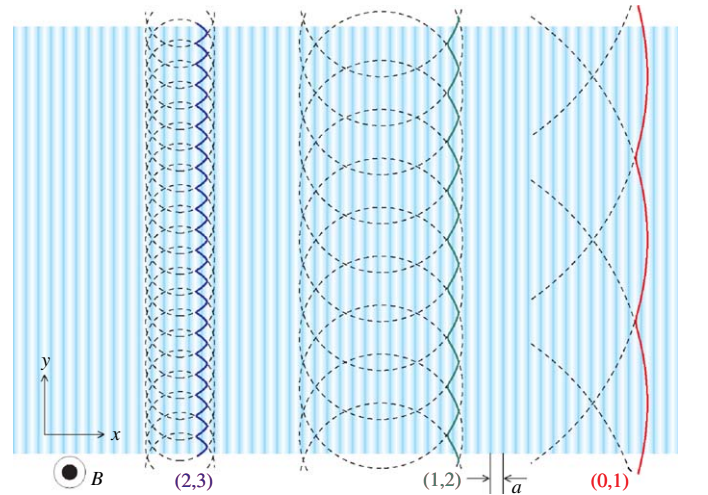


Fig. 3. Open orbits at resonance in the real space.

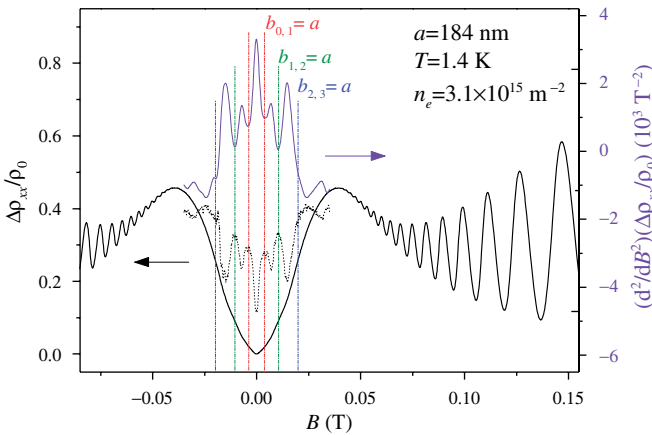


Fig. 1. Thick solid curve (left axis): low-field magnetoresistance $\Delta\rho_{xx}/\rho_0$ for ULSL with $a = 184$ nm, showing PMR and CO. Dotted curve: oscillatory part obtained by subtracting slowly varying background. Thin solid curve (right axis): second derivative, $(d^2/dB^2)(\Delta\rho_{xx}/\rho_0)$. Vertical dot-dashed lines indicate the positions of minima in $(d^2/dB^2)(\Delta\rho_{xx}/\rho_0)$ (maxima in the oscillatory part), which agree well with $B_{j-1,j}^{\text{res}}$ ($j = 1, 2, 3$) in Eq. (3).

above)

$$\Delta k_n = k_F \left[\sqrt{1 - \left(\frac{n}{\lambda}\right)^2} + \frac{\eta_n}{2} - \sqrt{1 - \left(\frac{n}{\lambda}\right)^2} - \frac{\eta_n}{2} \right] \simeq k_F \eta_n / 2 \quad (1)$$

with $k_F = \sqrt{2\pi n_e}$ the Fermi wave number, and $\lambda \equiv ak_F/\pi$ the number of minibands lying below the Fermi energy.

Electron trajectories in the real space are obtained by rotating by $\pi/2$ and multiplying by the factor \hbar/eB , as shown in Fig. 3. Electrons in an open orbit denoted by (j, k) tracks segments of cyclotron orbits, repeatedly diffracted alternately by the crystal momenta $2j\pi/a$ and $2k\pi/a$. Note that the crystal momentum $2j\pi/a$, or the gap between j th nearest Fermi circles, requires the j th harmonics of the potential modulation. The width of the orbit (j, k) reads, in the limit of small η_n (neglecting the gap width)

$$b_{j,k} = R_c \left[\sqrt{1 - (j/\lambda)^2} - \sqrt{1 - (k/\lambda)^2} \right] \quad (2)$$

with $R_c = \hbar k_F / e|B|$ the cyclotron radius. The condition for resonance is that the width equals multiples of the period, $b_{j,k} = va$. The simplest cases, $v = 1$, are shown in Fig. 3. The magnetic field at the resonance is therefore given by

$$|B_{j,k,v}^{\text{res}}| = \frac{\hbar k_F}{eva} \left[\sqrt{1 - (j/\lambda)^2} - \sqrt{1 - (k/\lambda)^2} \right]. \quad (3)$$

The minima in $(d^2/dB^2)(\Delta\rho_{xx}/\rho_0)$ was found to be well described by Eq. (3) for the ranges of a and n_e examined. As exemplified in Fig. 1, resonance ($v = 1$) of open orbits (0, 1), (1, 2), and (2, 3) were observed for ULSL with $a = 184$ nm, which indicates that the harmonic contents V_1 , V_2 , and V_3 are present in the potential modulation.

In general, the profile of potential modulation in ULSL having small period-to-depth ratio a/d ($a/d < \sim 2$ in our present samples) is considered to be simply sinusoidal $V(x) = V_1 \cos(2\pi x/a)$. This is because an effect exerted at the surface generally decays exponentially along the depth; the n th harmonics will decay as $\propto \exp(-2\pi nd/a)$, thereby leaving predominantly the fundamental component. In fact, CO shows excellent agreement with the formula taking only the fundamental component alone

$$\frac{\Delta\rho_{xx}^{\text{osc}}}{\rho_0} = \gamma A\left(\frac{\pi}{\mu_W B}\right) A\left(\frac{T}{T_{a,1}}\right) |B| \frac{V_1^2}{a} \sin\left(2\pi \frac{2R_c}{a}\right) \quad (4)$$

with γ and μ_W sample dependent parameters [10,11], as demonstrated in the main panel of Fig. 4. However, the observation of the geometric resonance involving higher harmonics discussed above forces us to reconsider the profile in our ULSL samples. We immediately find the presence of the second and the third harmonics in CO by performing a Fourier transform to the oscillatory part $\Delta\rho_{xx}/\rho_0$ (plotted against $1/B$), as shown in the inset of Fig. 4. Although the intensities of the higher harmonics in the spectrum are quite small, care should be taken in estimating the magnitude of the potential from the CO amplitude. For generic periodic potential modulation including higher harmonics, $V(x) = \sum_{n=1}^{\infty} V_n \cos(2\pi nx/a)$,

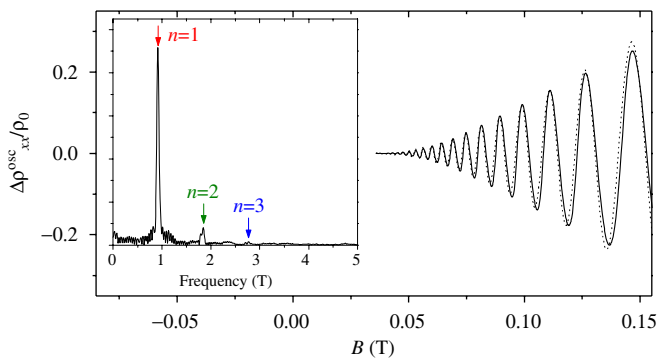


Fig. 4. Main panel: oscillatory part of CO obtained by subtracting slowly varying background from the experimental trace in Fig. 1 (solid trace) and calculated assuming a sinusoidal modulation $V(x) = V_1 \cos(2\pi x/a)$, Eq. (4) (dotted trace). Inset: Fourier spectrum of the solid trace in the main panel after replotted against $1/B$.

the CO is described by

$$\frac{\Delta\rho_{xx}^{\text{osc}}}{\rho_0} = \gamma A\left(\frac{\pi}{\mu_W B}\right) |B| \sum_{n=1}^{\infty} A\left(\frac{T}{T_{a,n}}\right) \frac{nV_n^2}{a} \sin\left(2\pi \frac{2R_c}{a/n}\right). \quad (5)$$

The n th harmonics are weighted by the thermal damping factor $A(T/T_{a,n})$, where $T_{a,n} = (1/2\pi^2)(\hbar k_F/2n)\hbar\omega_c/k_B$ with $A(x) \equiv x/\sinh(x)$. It can readily be verified that the factor $A(T/T_{a,n})$ becomes much smaller for larger n : the CO have lower sensitivity to higher harmonics. By an analogous argument, characteristic temperature T_λ for the open-orbit resonance are obtained by multiplying a large factor $2\sqrt{1 - (j/\lambda)^2} \sqrt{1 - (k/\lambda)^2} / [\sqrt{1 - (j/\lambda)^2} - \sqrt{1 - (k/\lambda)^2}]$ to $T_{a,1}$ and therefore the thermal damping factor is insensitive to indices j , k in the magnetic field and the temperature ($T \leq 4.2$ K) range of the present interest, rendering the sensitivity to higher harmonics higher compared with that of CO. Quantitative analyses of CO taking account of the thermal damping effect reveal that both V_2 and V_3 have an amplitude roughly 30% of that of $V_1 = 0.25$ meV, namely $V_2 \simeq V_3 \simeq 0.08$ meV, for our ULSL with $a = 184$ nm [11]. Possible reasons for V_2 , V_3 being larger than expected from the exponential decay are discussed in Ref. [11].

For the open orbits to be observed in a magnetic field, it is necessary for the electrons to survive the magnetic breakdown. The probability of breakdown for the n th minigap is given by [12] $p_n^{\text{bd}}(B) = \exp(-B_n^{\text{bd}}/B)$ with

$$B_n^{\text{bd}} = \frac{\pi m^* V_n^2 \lambda}{8\hbar e E_F n} \left[1 - \left(\frac{n}{\lambda}\right)^2 \right]^{-1/2}. \quad (6)$$

The probabilities for electrons to outlive the breakdown, $q_n^{\text{bd}}(B) = 1 - p_n^{\text{bd}}(B)$, are plotted in Fig. 5 as a function of B for sample parameters of the ULSL shown in Fig. 1. Small but finite probability remains for the survival of $n = 2$ and 3 minigaps, allowing for open orbits involving the harmonics to be observed.

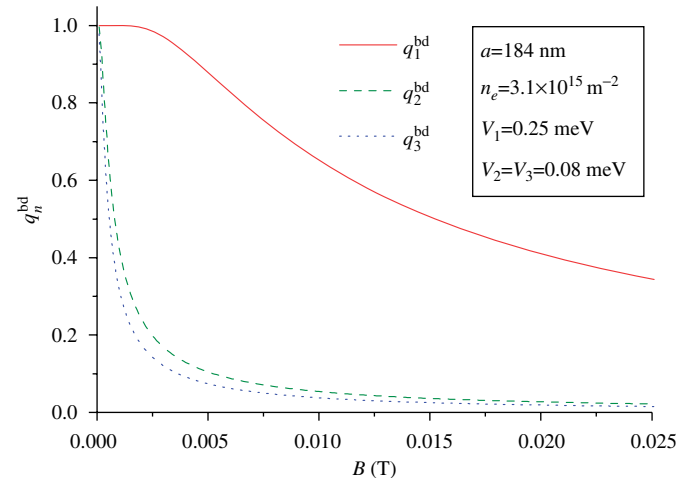


Fig. 5. Probabilities for electrons in open orbits to survive the magnetic breakdown.

Finally, we discuss the dependence of the intensity of the resonance on B . Although it is difficult to quantify the intensities owing to their smallness, Fig. 1 reveals that the amplitude first increases and then decreases with increasing B , with $b_{1,2} = a$ showing the largest amplitude. The competition of two factors, magnetic breakdown and scattering, seems to mainly govern the amplitude. Due to the magnetic breakdown, the amplitude is inclined to become smaller with increasing B . On the other hand, scattering will favor larger B . Electrons in an open orbit follow a periodic motion, as illustrated in Fig. 3. The distance an electron travels during one period in an open orbit $(j-1, j)$ is given by

$$L_j = 2R_j \{ \arcsin(j/\lambda) - \arcsin[(j-1)/\lambda] \} \quad (7)$$

with $R_j = \hbar k_F / e |B_{j-1,j,1}|$. Clearly, L_j decreases, hence the number of periods experienced by electrons before being scattered, L_s/L_j with L_s the mean free path, increases with increasing B , which will make the resonance more apparent. Considering the breakdown probability at both edges, the amplitude of resonance of an orbit $(j-1, j)$ will be roughly proportional to $q_{j-1}^{\text{bd}}(B) q_j^{\text{bd}}(B) \exp(-L_j/L_s)$ evaluated at $B = B_{j-1,j,1}^{\text{res}}$, which actually gives a larger value at $j=2$ than at $j=1$ and 3, using L_s derived from single electron scattering time.

To summarize, we have demonstrated that the open-orbit resonance is a sensitive probe to the small-amplitude

higher harmonics in the potential modulation of ULSL which cannot be detected by more conventional method employing CO unless careful analyses are performed.

This work was supported by MEXT KAKENHI (15540305, 13304025 and 12CE2004).

References

- [1] D. Weiss, K.V. Klitzing, K. Ploog, G. Weimann, *Europhys. Lett.* 8 (1989) 179.
- [2] P.H. Beton, E.S. Alves, P.C. Main, L. Eaves, M.W. Dellow, M. Henini, O.H. Hughes, S.P. Beaumont, C.D.W. Wilkinson, *Phys. Rev. B* 42 (1990) 9229.
- [3] L. Esaki, R. Tsu, *IBM J. Res. Dev.* 14 (1970) 61.
- [4] C. Albrecht, J.H. Smet, K. von Klitzing, D. Weiss, V. Umansky, H. Schweizer, *Phys. Rev. Lett.* 86 (2001) 147.
- [5] R.A. Deutschmann, W. Wegscheider, M. Rother, M. Bichler, G. Abstreiter, C. Albrecht, J.H. Smet, *Phys. Rev. Lett.* 86 (2001) 1857.
- [6] A. Endo, Y. Iye, *Phys. Rev. B* 71 (2005) 081303.
- [7] E. Skuras, A.R. Long, I.A. Larkin, J.H. Davies, M.C. Holland, *Appl. Phys. Lett.* 70 (1997) 871.
- [8] A. Endo, Y. Iye, in: J. Menéndez, C.G.V. de Walle (Eds.), *Physics of Semiconductors 2004. Proceedings of 27th International Conference on Physics Semiconductors*, AIP, New York, 2005, p. 1013.
- [9] J.C. Slater, *Phys. Rev.* 87 (1952) 807.
- [10] A. Endo, S. Katsumoto, Y. Iye, *Phys. Rev. B* 62 (2000) 16761.
- [11] A. Endo, Y. Iye, *J. Phys. Soc. Jpn.* 74 (2005) 2797.
- [12] P. Streda, A.H. MacDonald, *Phys. Rev. B* 41 (1990) 11892.